ISSN: 0067-2904

Examining the Seasonal Correlations Among Different Ionospheric Indices During Solar Cycle Twenty-Four

Aula A. Ezzat[1]*, Khalid A. Hadi[2]
[1]*Ministry of Scene and Technology, , Directorate of Space technology and Communication, Baghdad, Iraq.*
[2]*Department of Astronomy and Space, College of Science, University of Baghdad, Baghdad, Iraq.*

Received: 5/6/2023 Accepted: 4/9/2023 Published: 29/2/2024

Abstract

The present work aimed to examine the nature and degree of the cross-correlations among three different ionospheric indices: these are Optimum Working Frequency (OWF), Highest Probable Frequency (HPF), and Best Usable Frequency (BUF). VOCAP and ASASPS models were adopted to determine the datasets of the selected ionospheric indices. The determination was made for different transceiver stations that provide certain HF connection links during the minimum and maximum years of solar cycle 24, 2009 and 2014, respectively. Matlab program was implemented to produce the geodesic parameters for the selected transceiver stations. The determination was made for different path lengths (500, 1000, 1500, and 2000) Km and bearings (0^o, 45^o, 90^o ..... 315^o). Different correlation methods were used to examine the best determination coefficient values between the tested parameters. A third-order polynomial equation was set as the best correlation method that gave a better description for the correlation among the tested parameters. The proposed mathematical correlation equations were used to predict the seasonal values of the (HPF, OWF and BUF) parameters. The proposed equations were verified by comparing their values with the observed datasets during the study years. Also, the predicted values were tested using different statistical methods, which gave good results for all tested cases.

Keywords: HF Communication, Ionospheric Parameters, HPF, OWF, BUF, Cross-correlation

أختبار العلاقات التبادلية الموسمية بين معلمات الغلاف الأيوني المختلفة أثناء الدورة الشمسية الرابعة والعشرون

علا علاء عزت[1]*، خالد عبد الكريم هادي[2]
[1]وزارة العلوم والتكنولوجيا ، دائرة الفضاء والاتصالات ، بغداد ، العراق
[2]قسم الفلك والفضاء ، كلية العلوم ، جامعة بغداد ، بغداد ، العراق

الخلاصة

يهدف العمل الحالي إلى دراسة طبيعة ودرجة الترابط بين ثلاثة مؤشرات آيونوسفيرية مختلفة وهي Optimum Working Frequency (OWF) و Hiest Propable Frequency (HPF) و Best Usable Frequqncy (BUF)،تم استخدام نماذج VOCAP و ASASPS لحساب قيم البيانات للمؤشرات

*Email: aula1988@yahoo.com

الآيونوسفيرية المختارة. اجريت الحسابات لمحطات الإرسال / الاستقبال المختلفة التي توفر روابط اتصال عالية التردد خلال سنوات الصغرى والعظمى للدورة الشمسية 24 (2009 و 2014) على التوالي. تم تنفيذ برنامج Matlabلايجاد قيم المعلمات الجيوديسية لمحطات الإرسال / الاستلام لأطوال مسافات مختلفة (500، 1000، 1500 و 2000) كم واتجاهات مختلفة(0^o, 45^o, 90^o ..... 315^o). تم تطبيق طرق ارتباطية مختلفة لاختبار افضلها بين المعاملات المختبرة . تم اقتراح معادلات رياضية متعددة الحدود (الدرجة الثالثة) كأفضل طريقة تصف القيم الارتباطية بين المعاملات المحددة لغرض الدراسة. تمكنت المعادلات المقترحة من التنبؤ بالقيم الموسمية للمؤشرات (HPF) و(OWF) و (BUF).و تم التحقق منها من خلال مقارنتها مع قيم المعلمات المرصودة خلال سنوات الدراسة . كما تم اختبار القيم المتوقعة باستخدام طرق إحصائية مختلفة والتي قدمت نتائج جيدة لجميع الحالات المختبرة.

1. Introduction

The ionosphere, one of the upper atmosphere's layers, extends from (80 to 1000) km and higher [1]. When solar radiation interacts with chemical elements in the atmosphere, the electrically neutral layer of the ionosphere becomes ionized. This is done by displacing electrons from atoms and molecules [2]. The High-Frequencies HF (2 to 30) MHz are reflected back to Earth by the ionosphere, which makes it useful for long-distance communications (point-to-point communication). So, one of the most important parts of applying the technique of HF-radio system is frequency prediction which has been used to describe the optimum radio frequency values which are necessary to obtain radio communication between the transmitting and receiving stations. Therefore, HF prediction technology research and validation have become so significant that much-related work has been done since the 20th century [3].

High-frequency communications are particularly difficult during space weather events because the ionosphere, which is a dynamic propagation environment, deviates significantly from normal median behavior [4, 5]. As a result of variations in ionospheric variables (electron density for each layer) during the day, month, year, geographical location, and approximately 11-year sunspot cycle, additionally, the angle of incidence of the radio wave affects the values of the ionospheric predicted parameter, which are continually changing in the D, E, and F layers[5, 6]. Figure 1 shows the structure of the ionospheric layer during day and night times.

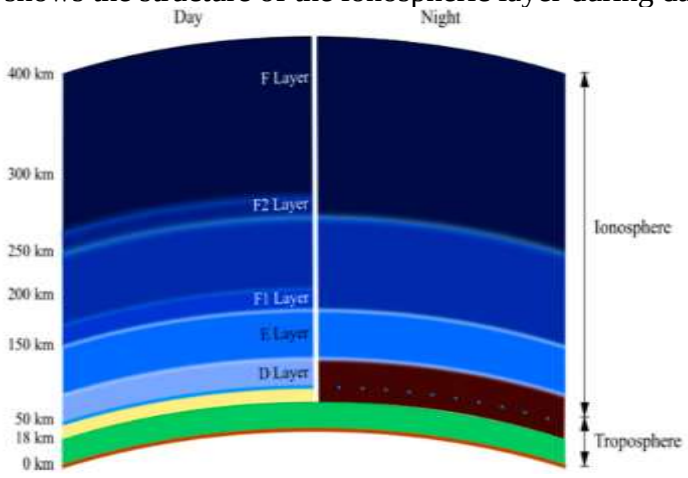

Figure 1: Ionospheric layer structure during day and night times [7].

Many researches and studies were developed to study HF radio communication parameters, like Malik, R. A., et al. (2014), who studied the relationship between sunspot number and the Maximum Usable Frequency (MUF) parameter. They found that there is a direct relationship between the studied parameters, where the sunspot number increases with increasing the range

of the MUF parameter [8]. Abdulkareem M. D., et al. (2016), studied the seasonal mutual correlation between the Maximum Usable Frequency (MUF), Optimum Working Frequency (OWF), and Lowest Useable Frequency (LUF) ionospheric parameters during the maximum and minimum years of solar cycle 24. They concluded that the seasonal mutual correlation between (MUF & OWF) parameters can be represented by a simple linear regression equation, while the seasonal correlated relationship between (MUF & LUF), (OWF & LUF) can be represented by a fourth-order polynomial equation (Quartic Polynomial Equation) [9]. Thabit S. A., et al. (2020), determined the seasonal Optimal Reliable Frequency (ORF) variations between different transmitter/receiver stations (Mosul, Baghdad, and Basra), which are located in the northern, center, and southern of Iraq. They concluded that the ORF value increased with increasing path length and varied with different bearing values. Additionally, they found that the seasonal ORF values were higher at the peak of solar cycle 24 than at the minimum of the cycle [10].

The objective of this study is to examine the seasonal correlations among three different ionospheric parameters: Optimum Working Frequency (OWF), Highest Probable Frequency (HPF), and Best Usable Frequency (BUF) that provide certain HF connection links between various transceiver stations during the minimum and maximum years of solar cycle 24.

2. Ionospheric Communication Parameters

Since the ionosphere is always variable, radio signals (HF communications signals) are affected differently depending on their frequencies. The ionospheric parameter determines the optimum range of frequencies (HF) reflected from the ionospheric layers between two terminals at a certain moment. There are many important parameters in HF ionospheric communications that can be used to maintain the connection links between two terminals [11-13]. Following are the definitions of some ionospheric communications parameters that will be adopted in this research:

- **The Optimum Working Frequency (OWF)**

The Optimum Working Frequency (OWF), also known as FOT (Frequency of Optimum Transmission), represents the highest effective frequency predicted to be usable for a specified path of a particular circuit for 90% of the days in a month. The estimated OWF can exceed approximately 85% of the Maximum Usable Frequency (MUF) [4, 11]. The MUF refers to the highest frequency at which radio waves are reflected back to Earth by the ionosphere [13].

- **The Highest Probable Frequency (HPF)**

In accordance with the highest frequency (HPF), at which radio waves may be utilized to communicate across a specified path and at a given time under specific ionospheric circumstances, the upper usable limit exceeds 10% of the time, or 3 days per month, or in other words, in exceptional conditions [14, 15].

- **The Best Usable Frequency (BUF)**

The Best Usable Frequency (BUF) refers to the frequency at which a radio wave can be transmitted and received most effectively over a given distance at a particular time. It can be defined as the frequency from a specified set that offers a maximum signal-to-noise ratio (S/N) while also satisfying the specified minimum take-off angle, required S/N ratio, and probability level [12].

3. Methods and Calculation

In this study, Baghdad city (Lat. 33.35° N, Long. 44.42° E) was adopted as a transmitter station (T_x), while other thirty-two locations were chosen around the transmitter station to represent receiving stations (R_x). The geographical coordinates (Longitude and Latitude) of the receiver stations were determined based on various geodesic parameters, including path lengths of (500, 1000, 1500, and 2000) km and bearings at (0 °, 45°, 90°, … and 315°). The determination of these parameters was performed using a program that was designed and implemented using Matlab programming language. Equations (1) and (2) were used to calculate the geographical location coordinates of the receiving stations [16, 17]. Table 1 presents the determined geographical coordinates for the specific receiving locations that were chosen.

$$\varphi_2 = \text{asin}(sin\varphi_1\, cos\,\delta + cos\,\varphi_1\, sin\,\delta\ cos\,\theta) \quad (1)$$

$$\lambda_2 = \lambda_1 + atan2(\sin\theta \sin\delta \cos\varphi 1\,, \cos\delta - \sin\varphi 1 \sin\varphi 2) \quad (2)$$

Where: φ : latitude
λ : longitude
θ : the bearing (clockwise from north)
δ : the angular distance d/R
d : path length
R : Earth's radius (6,371 km)

Table 1: The determined geographical coordinates (latitudes and longitudes) for the specific geodesic parameters (path length and bearing) of the receiving stations distributed around the transmitting station (Baghdad city)

Receiver Stations (R_x)	Path length	Bearing	Latitude (N)	Longitude (E)	Locations of R_x Stations
BGN5	500	0	37.846	44.420	Iran , Dustan
BGNE5		45	36.467	48.372	Iran, Zarian Abad
BGE5		90	33.233	49.798	Iran , Aligudaraz
BGSE5		135	30.116	48.095	Iraq, Basra
BGS5		180	28.853	44.420	Saudi Arabia, Hafar Al Batin
BGSW5		225	30.116	40.745	Saudi Arabia, Sakaka
BGW5		270	33.234	39.042	Iraq
BGNW5		315	36.468	40.467	Syria , Kizwan Dagi
BGN10	1000	0	42.343	44.420	Georgia , Midelaani
BGNE10		45	39.444	52.649	Caspian Sea
BGE10		90	32.887	55.148	Iran , Poshte Badam
BGSE10		135	26.786	51.533	Arabian Gulf
BGS10		180	24.356	44.420	Saudi Arabia, Al Duwadimi
BGSW10		225	26.786	37.307	Saudi Arabia , Bejeal
BGW10		270	32.888	33.692	Mediterranean Sea
BGNW10		315	39.444	36.191	Turkey, Sivrailan
BGN15	1500	0	46.840	44.420	Russia , Ovaia Oaara
BGNE15		45	42.250	57.295	Uzbekistan, Saygamsh Lake
BGE15		90	32.315	60.443	Iran , Doroh
BGSE15		135	23.378	54.772	United Arab Emirates
BGS15		180	19.860	44.420	Saudi Arabia, Al Qirah
BGSW15		225	23.378	34.068	Egypt
BGW15		270	32.31	28.40	Mediterranean Sea

BGNW15		315	42.250	31.544	Black Sea
BGN20	2000	0	51.336	44.420	Russia, Mikhailovka
BGNE20		45	44.852	62.358	Kazakhstan
BGE20		90	31.526	65.659	Afghanistan, Bazarcheh
BGSE20		135	19.907	57.848	Oman, Arabian sea
BGS20		180	15.363	44.420	Yemen, Maayin
BGSW20		225	19.907	30.992	Sudan
BGW20		270	31.526	23.181	Libya
BGNW20		315	44.852	26.481	Romania

In this study, Voice of America Communication Analysis and Prediction (VOCAP) model (Version 08.0121W) was used to generate the datasets of the (HPF, OWF) ionospheric parameters, while the datasets of the (BUF) parameter was generated using Advanced Stand Alone Prediction System (ASAPS) model (Version 6.2.1). These parameters datasets were generated based on the monthly mean sunspot number (SSN) for the years 2009 (representing the minimum year of solar cycle 24) and 2014 (representing the maximum year of solar cycle 24), respectively. Table 2 presents the values of the monthly mean SSN for the years 2009 and 2014.

Table 2: Monthly mean SSN of the years 2009 and 2014 [18]

Month	Min. year (2009)	Max. year (2014)
Jan.	1.3	117
Feb.	1.2	146.1
Mar.	0.6	128.7
Apr.	1.2	112.5
May.	2.9	112.5
Jun.	6.3	102.9
Jul.	5.5	100.2
Aug.	0.0	106.9
Sep.	7.1	130
Oct.	7.7	90
Nov.	6.9	103.6
Dec.	16.3	112.9

The monthly predicted HPF and OWF ionospheric parameter values generated using VOCAP model showed a smooth behavior, while the BUF parameter values generated depending on the ASAPS model fluctuated according to the observed conventional measurements. Therefore, to standardize the monthly behavior of the three tested ionospheric parameters and to overcome these fluctuations, the predicted BUF values were smoothed mathematically to remove the irregular behavior of the data to obtain the smooth underlying trend.

In order to examine the seasonal correlation among the three tested ionospheric parameters (OWF, HPF, and BUF), the seasonal average of the monthly dataset values was calculated for the four seasons (Winter, Spring, Summer, and Autumn) during the minimum and maximum years of solar cycle 24 (2009 and 2014, respectively). The calculations were made depending on different geodesic path length and bearing values. Samples for the behavior of the seasonal variations of the three tested ionospheric parameters for the four seasons of the years 2009 and 2014 - solar cycle 24 were shown in Figure 2.

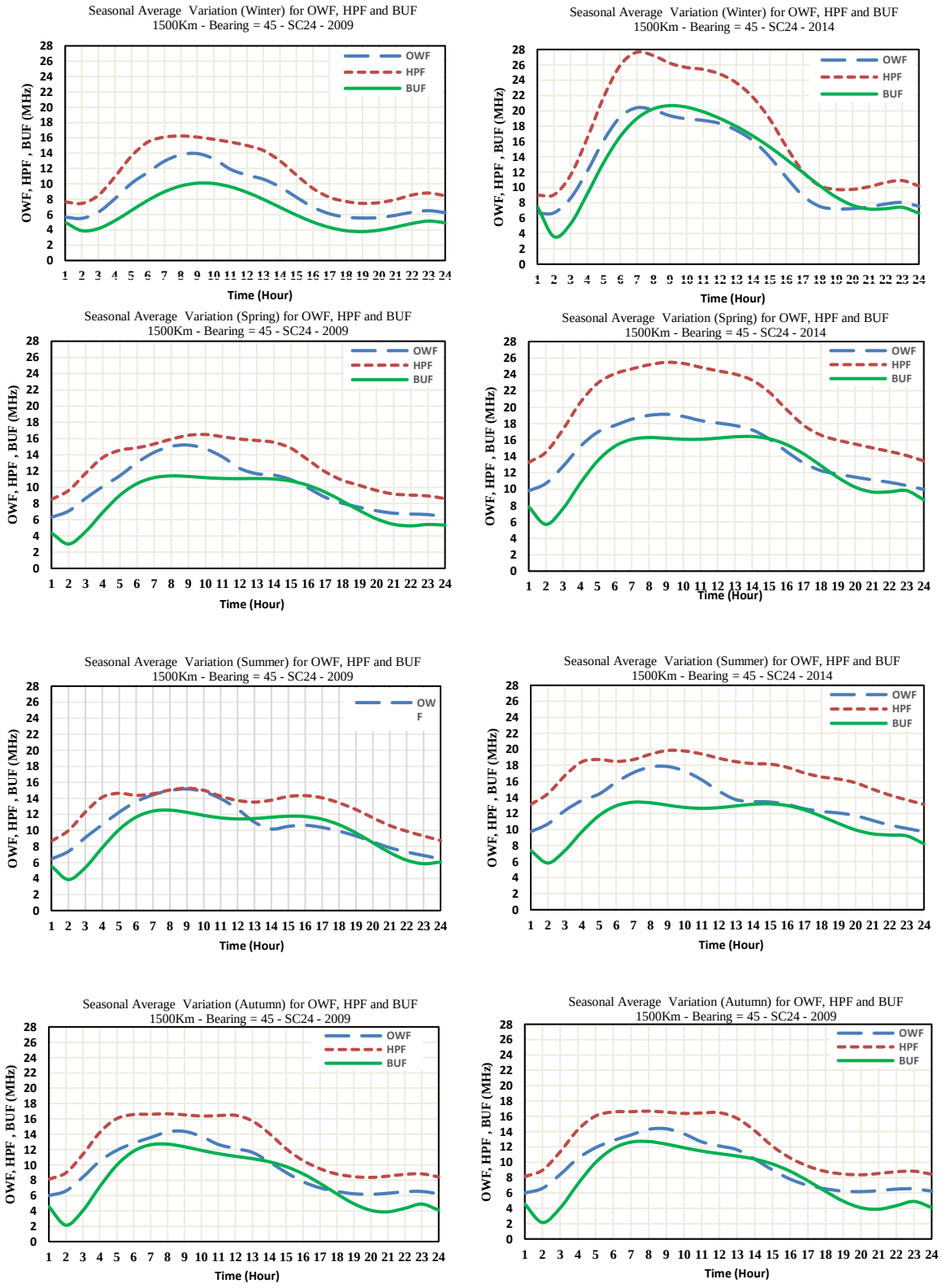

Figure 2: Samples of the seasonal variation behavior of the OWF, HPF, and BUF parameters values generated using VOCAP and ASAPS models for the minimum and maximum years of solar cycle 24 (2009 and 2014), respectively.

4. Results and Discussion

To determine the nature and degree of the seasonal correlation among HPF, OWF, and BUF parameters, different cross-correlation methods were applied, including exponential, linear, logarithmic, polynomial (second and third order), and power methods. The cross-correlation exams were performed mutually for each pair of parameters [OWF(BUF), OWF(HPF), HPF(OWF), HPF(BUF), BUF(OWF), and BUF(HPF)] for the two studied years and for all selected locations depending on the adopted geodesic parameters (path lengths (500, 1000, 1500, and 2000) km and bearings (0 °, 45°, 90°, … and 315°)).

The examination results for the seasonal cross-correlation methods between the tested parameter pairs were determined (type and order) depending on the highest determination coefficient value (R^2) (see Table 3, which illustrates the range of the correlation strength based on the value of (R^2)). Tables 4 and 5 show samples of the examination results for the seasonal correlation study between the tested parameters during the two tested years of solar cycle 24.

Table 3: Strength of correlation - determination coefficient

Determination Coefficient (R^2) range	Type of correlation
≤ 0.25	**No correlation**
0.25 to 0.5	**Weak correlation**
0.5 to 0.75	**Moderated correlation**
0.75 to 1	**Good correlation**

Table 4: Examination results of the seasonal correlation between the studied parameters for the year 2009 based on the determination coefficient (R^2) value

		Determination coefficient (R^2) Path 500 Km_ Bearing 315°_SC 24_2009.					
OWF(HPF)		Exp.	Linear	Log.	Polynomial 2nd order	Polynomial 3rd Order	power
Bearing (315°)	Winter	0.9921	0.9994	0.9931	0.9994	**0.9995**	0 .9994
	Spring	0.9905	0.9990	0.9914	0.9990	**0.9991**	0.9993
	Summer	0.9668	0.9543	0.9465	0.9546	**0.9556**	0.9691
	Autumn	0.9939	0.9998	0.9932	**0.9999**	0.9999	0.9998
		Determination coefficient (R^2) Path 1000 Km_ Bearing135 °_SC 24_2009.					
BUF(OWF)		Exp.	Linear	Log.	Polynomial 2nd order	Polynomial 3rd Order	power
Bearing (135°)	Winter	0.8597	0.9194	0.9095	**0.9203**	0.9203	0.8829
	Spring	0.7243	0.7194	0.7652	0.8099	**0.8122**	0.7778
	Summer	0.6749	0.6988	0.7525	**0.7966**	0.7966	0.735
	Autumn	0.7365	0.8183	0.8524	0.8614	**0.8624**	0.7826
		Determination coefficient (R^2) Path 1500 Km_ Bearing 270°_SC 24_2009.					
OWF(BUF)		Exp.	Linear	Log.	Polynomial 2nd order	Polynomial 3rd Order	power
Bearing (270°)	Winter	0.8828	0.9349	0.9383	0.9446	**0.9460**	0.9111
	Spring	0.9202	0.8936	0.8485	0.8952	**0.9085**	0.8957
	Summer	0.8542	0.8189	0.7722	0.8494	**0.8666**	0.8238

	Autumn	0.9356	0.9255	0.8414	**0.9566**	0.9566	0.8747
Bearing (180°)	**BUF(HPF)**	**Determination coefficient (R^2) Path 2000 Km_ Bearing180 °_SC 24_2009.**					
		Exp.	Linear	Log.	Polynomial 2nd order	Polynomial 3rd Order	power
	Winter	0.6699	0.8857	0.9084	0.9022	**0.9096**	0.7446
	Spring	0.8715	0.9228	0.9129	**0.9240**	0.9240	0.906
	Summer	0.8429	0.8908	0.9175	0.9242	**0.9256**	0.8917
	Autumn	0.7219	0.8729	0.8834	0.8823	**0.8850**	0.7731

Table 5: Examination results of the seasonal correlation between the studied parameters for the year 2014 based on the determination coefficient (R^2) value.

Bearing (270°)	**OWF(BUF)**	**Determination coefficient (R^2) Path 500 Km _Bearing 270° _SC 24_2014.**					
		Exp.	Linear	Log.	Polynomial 2nd order	Polynomial 3rd Order	power
	Winter	0.9056	0.8529	0.7459	0.9133	**0.9189**	0.8302
	Spring	0.9302	0.9375	0.9091	**0.9411**	0.9411	0.9233
	Summer	0.8816	0.8745	0.8219	0.9079	**0.9089**	0.8387
	Autumn	0.9301	0.9132	0.8589	**0.9305**	0.9305	0.8986
Bearing (90°)	**BUF(OWF)**	**Determination coefficient (R^2) Path 1000 Km_Bearing 90° _SC 24_2014.**					
		Exp.	Linear	Log.	Polynomial 2nd order	Polynomial 3rd Order	power
	Winter	0.7522	0.9047	0.9118	0.9098	**0.9186**	0.7954
	Spring	0.8244	0.8685	0.8769	0.8783	**0.8795**	0.8438
	Summer	0.6381	0.6397	0.6859	0.7793	**0.7803**	0.6871
	Autumn	0.8529	0.9026	0.9097	0.9091	**0.9107**	0.876
Bearing (270°)	**OWF(BUF)**	**Determination coefficient (R^2) Path 500 Km _Bearing 270° _SC 24_2014.**					
		Exp.	Linear	Log.	Polynomial 2nd order	Polynomial 3rd Order	power
	Winter	0.9056	0.8529	0.7459	0.9133	**0.9189**	0.8302
	Spring	0.9302	0.9375	0.9091	**0.9411**	0.9411	0.9233
	Summer	0.8816	0.8745	0.8219	0.9079	**0.9089**	0.8387
	Autumn	0.9301	0.9132	0.8589	**0.9305**	0.9305	0.8986
Bearing (90°)	**BUF(OWF)**	**Determination coefficient (R^2) Path 1000 Km_Bearing 90° _SC 24_2014.**					
		Exp.	Linear	Log.	Polynomial 2nd order	Polynomial 3rd Order	power
	Winter	0.7522	0.9047	0.9118	0.9098	**0.9186**	0.7954
	Spring	0.8244	0.8685	0.8769	0.8783	**0.8795**	0.8438
	Summer	0.6381	0.6397	0.6859	0.7793	**0.7803**	0.6871
	Autumn	0.8529	0.9026	0.9097	0.9091	**0.9107**	0.876

The results presented in tables 4 and 5 highlight the seasonal cross-correlation examination of the presented and predicted datasets for the three tested ionospheric parameters. It was noticed

that the (OWF-HPF) indices exhibited a stronger correlation compared to the correlations between the (OWF-BUF) and (HPF-BUF) indices. Additionally, the seasonal examination results indicated that there was a good seasonal cross-correlation among the three tested parameters during the seasonal times (winter, spring, and autumn), while the cross-correlation was rather weak during the summer season.

Based on the seasonal cross-correlation examination results, the seasonal correlation equation that can accurately describe the nature and degree of the cross-correlation among the tested pairs of parameters was achieved. The examination results showed that the best mathematical equation that could give a better description of the cross-correlation between the tested ionospheric parameters was a polynomial equation, which can be described by the following formula:

$$y = \sum_{i=1}^{\infty} k_i x^i \quad \ldots\ldots\ldots (3)$$

$$y = k_0 + k_1 x + k_2 x^2 + k_3 x^3 + k_i x^i \quad \ldots\ldots\ldots (4)$$

Depending on the calculated determination coefficient (R^2) values that were obtained from the examination results of the seasonal correlation between the studied parameters, the third-order polynomial equation showed a stronger correlation between the tested parameters. Therefore, the proposed cross-correlation formulas among the investigated parameters may be represented by the following set of equations:

$$\left.\begin{aligned} HPF &= \sum_{i=1}^{\infty} K_i (OWF)^i \\ OWF &= \sum_{i=1}^{\infty} K_i (HPF)^i \\ HPF &= \sum_{i=1}^{\infty} K_i (BUF)^i \\ BUF &= \sum_{i=1}^{\infty} K_i (HPF)^i \\ OWF &= \sum_{i=1}^{\infty} K_i (BUF)^i \\ BUF &= \sum_{i=1}^{\infty} K_i (OWF)^i \end{aligned}\right\} \quad \ldots\ldots\ldots (5)$$

Where: $k_i = c$orrelation coefficient for the (i^{th}) order of the polynomial equation.

To examine the accuracy of the proposed mathematical formulas, the seasonal values of the HPF, OWF, and BUF parameters were calculated using the suggested correlated equations for the four seasons of the years 2009 and 2014, and for all adopted geodetic conditions. The generated datasets were compared with the predicted seasonal ionospheric parameter values. Figures 3 and 4 show different comparison samples of the ionospheric parameter datasets generated using the proposed equations with the predicted values of the studied parameter

calculated using VOCAP and ASAPS models, for the seasonal times of the minimum and maximum years of the 24 solar cycle.

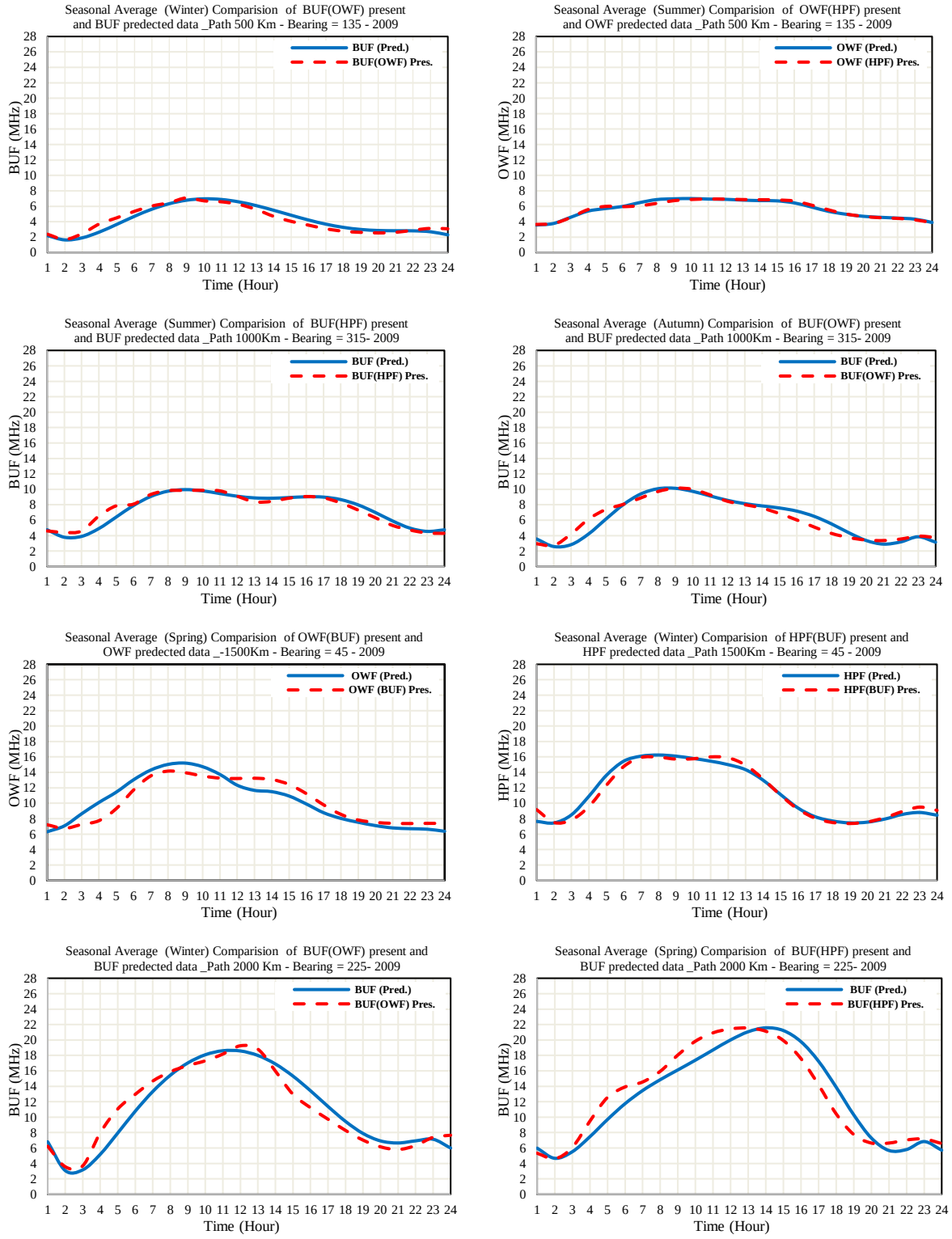

Figure 3 : Samples of a comparison between the generated datasets using the suggested equations for the studied parameters with the predicted values of the parameters, for the seasonal times of the minimum year of solar cycle 24 (year 2009).

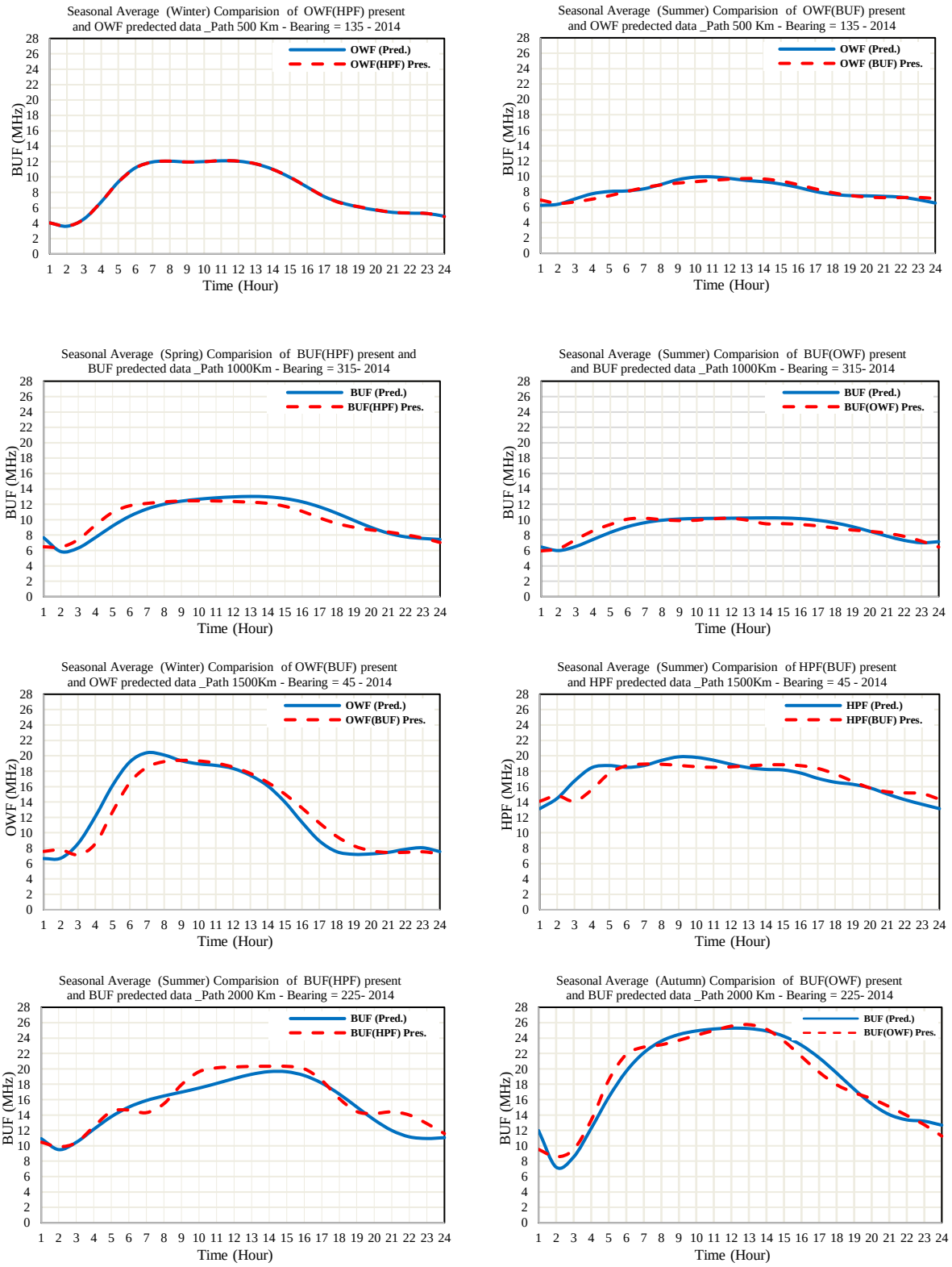

Figure 4 - Samples of a comparison between the generated datasets using the suggested equations for the studied parameters with the predicted values of the parameters, for the seasonal times of the maximum year of solar cycle 24 (year 2014).

In order to examine the accuracy of the generated results of the three ionospheric parameters using the proposed mathematical equations compared to the predicted dataset computed using

the selected ionospheric models, a statistical study of the minimum and maximum years of solar cycle 24 was conducted using a number of statistical analysis methods including, Normalized Root Mean Square Error (NRMSE), Determination Coefficient (R^2), and Mean Difference.

The results of the statistical calculations for the generated seasonal values using suggested formulas showed good agreement with the predicted ionospheric model values for all seasons and geodesic locations parameters (path length and bearing) of the study years (2009 and 2014) of solar cycle 24. Tables 6 and 7 present samples of the statistical calculation results that were conducted for the seasonal times of the two tested years of solar cycle 24 for different geodetic conditions.

Table 6: Samples of the statistical calculations results for the seasonal times of the minimum year (2009) of SC 24, for different Path length and different Bearings

Path length: 500 km				
	OWF(BUF)	NRMSE	Det. Coeff. (R^2)	Mean Diff.
Bearing(45°)	Winter	0.0679	0.9464	-0.0038
	Spring	0.0640	0.9270	-0.0138
	Summer	0.0759	0.7754	-0.0039
	Autumn	0.0916	0.8863	-0.0017

Path length: 1000 km				
	BUF(OWF)	NRMSE	Det. Coeff. (R^2)	Mean Diff.
Bearing(180°)	Winter	0.1177	0.9150	-0.0131
	Spring	0.1674	0.8155	0.0264
	Summer	0.1321	0.79600	0.0052
	Autumn	0.1150	0.8504	-0.0289

Path length: 1500 km				
	BUF (HPF)	NRMSE	Det. Coeff. (R^2)	Mean Diff.
Bearing(270°)	Winter	0.0760	0.9657	-0.0951
	Spring	0.0704	0.9676	-0.1135
	Summer	0.0927	0.9041	0.0601
	Autumn	0.1106	0.9267	-0.0545

Path length: 2000 km				
	HPF(BUF)	NRMSE	Det. Coeff. (R^2)	Mean Diff.
Bearing(270°)	Winter	0.0679	0.9616	-0.0207
	Spring	0.0593	0.9577	-0.0792
	Summer	0.0715	0.8438	-0.0410
	Autumn	0.0835	0.9360	-0.0159

Table 7: Samples of the statistical calculations results for the seasonal times of the maximum year (2014) of SC 24, for different Path length and different Bearings

Path length: 500 km				
	OWF(BUF)	NRMSE	Det. Coeff. (R^2)	Mean Diff.
Bearing (270°)	Winter	0.0976	0.9204	0.0084
	Spring	0.0701	0.8529	-0.0814
	Summer	0.0328	0.9245	0.0096
	Autumn	0.0664	0.9363	-0.0019

Path length: 1000 km				
	BUF(OWF)	NRMSE	Det.Coeff. (R2)	Mean Diff.
Bearing (180°)	Winter	0.0938	0.9266	0.0392
	Spring	0.0797	0.8869	0.1046
	Summer	0.0814	0.8216	0.0373
	Autumn	0.0726	0.9502	-0.0463

Path length: 1500 km				
	BUF(HPF)	NRMSE	Det. Coeff. (R^2)	Mean Diff.
Bearing ((90°)	Winter	0.1359	0.8814	0.2471
	Spring	0.0826	0.8973	-0.2560
	Summer	0.0716	0.8186	-0.1611
	Autumn	0.1235	0.8850	-0.3520

Path length: 2000 km				
	HPF(BUF)	NRMSE	Det. Coeff. (R^2)	Mean Diff.
Bearing(315°)	Winter	0.1256	0.8936	-0.0620
	Spring	0.0805	0.8228	-0.1861
	Summer	0.0421	0.8269	0.0451
	Autumn	0.0968	0.8695	0.1739

5. Conclusions:

1. The three tested parameters, HPF, OWF, and BUF, exhibit similar behavior patterns over all seasons of the two tested years and for all distances and bearings that were selected for this study. The behavior of these parameters can be characterized based on their values: after sunrises, the values of HPF, OWF, and BUF ionospheric parameters increase, peaking at midday. Then after, at sunset, the parameter values begin to decrease due to a reduction in the electron density of the ionosphere layers.
2. The ionospheric parameters (HPF, OWF, and BUF) exhibited higher seasonal values in 2014 when solar activity reached its peak, as indicated by the average sunspot number (SSN) values. In contrast, their values were lower in 2009 when solar activity was at its minimum level, representing the lowest point of solar cycle 24.
3. The results of the seasonal cross-correlation exam among the three tested parameters showed that the seasonal cross-correlation between the two indices (OWF-HPF) was stronger than the correlation between (OWF-BUF) and (HPF-BUF) ionospheric parameters.
4. The examination results of this study indicated that there was a strong seasonal cross-correlation among the three tested parameters during the seasonal times (winter, spring, and autumn), while the cross-correlation between the mutual parameters was rather weak during the summer season.
5. The examination results of the seasonal cross-correlation showed that the mathematical equation that could give a better description of the seasonal cross-correlation among the tested ionospheric parameters was a third-order polynomial equation.
6. The results of the statistical calculations indicated that the data generated from the proposed mathematical equations showed a good agreement and closely matched the predicted data generated using the two international HF communication models (VOCAP & ASAPS). These models were adopted in the present study for the three parameters across all tested seasons, path-length, and bearings of the study years (2009 and 2014) of solar cycle 24.

Refrences:

[1] K. A. Difar and A. S. Tasu, "Investigation in Communication Behavior of Ionosphere Regions," *The Eighteenth International Conference on Networks*, vol. Copyright (c) IARIA, 2019.

[2] M. J. Jafar and K. A. Hadi, "Investigating the Compatibility of IRI and ASAPS Models in Predicting the foF2 Ionospheric Parameter over the Mid Latitude Region," *Iraqi Journal of Science*, vol. 62, no. 10, pp. 3759-3771, 2021.https://doi.org/10.24996/ijs.2021.62.10.34.

[3] M. Pietrella and M. Pezzopane, "Maximum usable frequency and skip distance maps over Italy," *Advances in Space Research*, vol. 66, no. 2, pp. 243-258, 2020.https://doi.org/10.1016/j.asr.2020.03.040.

[4] K. A. Hadi and M. D. Abdulkareem, "The Suggested Reciprocal Relationship between Maximum, Minimum and Optimum Usable Frequency Parameters Over Iraqi Zone," *Baghdad Science Journal*, vol. 17, no. 3, pp. 1058-1070, 2020.http://dx.doi.org/10.21123/bsj.2020.17.3(Suppl.).1058.

[5] A. K. Hassan, "Radio Contact Establishment Out of Iraqi Boarder using Nicosia Ionosonde Real data," *Iraqi Journal of Electrical Electronic Engineering* vol. 14, no. 2-2018, 2018.

[6] A. A. Temur and A. F. Ahmed, "Investigation of the Electron Coefficients of (Ar, He, N2, O2) Gases in the Ionosphere," *Baghdad Science Journal*, vol. 19, no. 6 (Suppl.), pp. 1558-1558, 2022.https://dx.doi.org/10.21123/bsj.2022.7296.

[7] J. J. Barona Mendoza, C. F. Quiroga Ruiz, and C. R. Pinedo Jaramillo, "Implementation of an Electronic Ionosonde to Monitor the Earth's Ionosphere via a Projected Column through USRP," *Sensors*, vol. 17, no. 5, p. 946, 2017. https://doi.org/10.3390/s17050946.

[8] R. Malik, M. Abdullah, S. Abdullah, and M. Homam, "The influence of sunspot number on high frequency radio propagation," in *2014 IEEE Asia-Pacific Conference on Applied Electromagnetics (APACE)*, 2014, pp. 107-110: IEEE

[9] M. D. Abdulkareem and K. A. Hadi, "Empirical Mutual Correlation Formula for Seasonal Ionospheric Parameters Variation Over Middle East Region " *International Journal of Advanced Research (IJAR)*, vol. 4, pp. 60-71, 2016.http://dx.doi.org/10.21474/IJAR01/1186

[10] S. A. Thabit, L. E. George, and K. A. Hadi, "Seasonal Variations of the Optimum Reliable Frequencies during Maximum and Minimum Periods of Solar Cycle 24," *Al-Mustansiriyah Journal of Science*, vol. 31, no. 4, pp. 15-27, 2020.https://doi.org./10.23851/mjs.v31i4.887.

[11] K. A. Hadi and A. Z. Azeez, "Analytical Investigation of the Seasonal Ionospheric Propagation Parameters Variation over Iraqi Area," *International Journal of Physics and Astronomy*, vol. 26, no. 2, 2013.

[12] S. A. Thabit, K. A. Hadi, and L. E. George, "Determination of the Annual Optimal Reliable Frequency for Different Transmitter/Receiver Stations Distributed over the Iraqi Territory," *Iraqi Journal of Science*, vol. 62, no. 4, pp. 1386-1395, 2021.https://doi.org/10.24996/ijs.2021.62.4.34.

[13] R. A. Nasser and K. A. Hadi, "Study the Impact of the Distance Factor on the Optimal Workable Frequencies for the Long Distance Radio Communications," *Iraqi Journal of Science*, vol. 56, no. 3B, pp. 2392-2400, 2015.

[14] K. A. Hadi and A. Z. Aziz, "The Suggested Correlation Formula between (HPF) and (OPMUF) Parameters over Middle East Region," *IOSR Journal of Electronics and Communication Engineering* vol. 1, pp. 36-44, 2012.http://dx.doi.org/10.9790/2834-0153644.

[15] T. O. V. BlogUpdated. (2018). *Getting the best operating frequency from VOACAP P2P predictions*. Available: https://voacap.blogspot.com/search?q=HPF

[16] I. S. D.-d. Websites. *Calculate distance, bearing and more between Latitude_Longitude points*. Available: http://www.movable-type.co.uk/scripts/latlong.html

[17] t. f. e. Wikipedia. *Great-circle distance*. Available: https://en.wikipedia.org/wiki/Great-circle_distance

[18] *World Data Center for the production_Sunspot Number*. Available: https://www.sidc.be/silso/datafiles